Improved Sliding Mode Control and Active Damping for LCL-filtered Voltage Source Inverter Connected to Distorted Grid

Amir Rabbani, Mohammad Mardaneh, Ehsan Jamshidpour, Philippe Poure

Improved Sliding Mode Control and Active Damping for LCL-filtered Voltage Source Inverter Connected to Distorted Grid

Amir Rabbani
Department of Electrical Engineering
Shiraz university of technology
Shiraz, Iran
A.rabbani@sutech.ac.ir

Mohammad Mardaneh
Department of Electrical Engineering
Shiraz university of technology
Shiraz, Iran
mardaneh@sutech.ac.ir

Ehsan Jamshidpour
Université de Lorraine-GREEN
F-54000 Nancy, France
ehsan.jamshidpour@univ-lorraine.fr

Philippe Poure
Université de Lorraine-IJL
F-54000 Nancy, France
philippe.poure@univ-lorraine.fr

***Abstract*—Grid-tied voltage source inverters (VSIs) with LCL filters are a promising solution for transmitting renewable energy to the grid, but they have a high tendency to resonance. To address this issue, various control techniques have been explored. This study proposes a sliding mode control with proportional-resonant (PR) control for LCL grid-tied inverters (GTIs). A PR controller is used to generate the reference capacitor voltage, eliminating the need for a derivative operation that is not always preferred in control methodologies. A sliding mode observer is also proposed to reduce sensor requirements and enhance system stability. The proposed method is evaluated for an inverter connected to an unbalanced network experiencing voltage fluctuations, s well, a nd s ag. T he e ffectiveness o f t he m ethod is demonstrated through simulation using Matlab/Simulink.**

***Index Terms*—Grid-tied inverter, LCL filter, P R c ontrol, Sliding mode controller, Sliding mode observer, VSI.**

I. Introduction

Voltage source inverters (VSIs) are commonly used in grid-tied inverter (GTI) applications to meet the demand for renewable energy sources [1]. However, the Pulse Width Modulation (PWM) switching harmonics generated by VSIs need to be mitigated with a filter t o c omply w ith r equisite s tandards and achieve a sinusoidal current between the inverter and grid [1]. LCL filters o ffer s everal a dvantages o ver L fi lters, su ch as significantly b etter a ttenuation c apabilities a t l ower switching frequencies and smaller inductance size [2]. However, the use of LCL filters p oses i nherent c omplexities f rom a control perspective that arise from resonance issues between filter components, leading to the introduction of complex-conjugate poles that can spoil system stability [2]. Hence, identifying an appropriate control strategy to ensure desirable system dynamics is a crucial task.

To mitigate the effects of resonance in the LCL filter, two broad categories of damping solutions have been implemented: passive damping and active damping. Passive damping involves the insertion of small valued resistors into the LCL filter, providing an easy but inefficient approach to damping [3]. Active damping, on the other hand, utilizes virtual resistors and requires additional sensors for voltage or current measurement. Despite its increased reliability, active damping is subjected to instability due to the fluctuating parameters of the grid and the varying resonance frequency [3], [4].

Proportional-Integral (PI) controllers are a typical and straightforward method to regulate the current loop of an LCL GTI [5]. However, they have some drawbacks, including stability issues as well as complications with reference tracking. The implementation of PR controllers could significantly improve the converter's reference tracking and mitigate known shortcomings typically associated with traditional PI controllers [5]. Non-linear controllers, such as Sliding Mode Controllers (SMCs), have been shown to have appealing features such as fast dynamic response and robustness against parameter variation compared to traditional controllers [3], [6], [7]. SMCs, especially the Super Twisting Sliding Mode Observer (STSMO) with SMC, have been utilized for variable structure systems such as GTI because of their fast convergence rate, strong robustness to external disturbances, and suitable steady-state characteristics [8], [9].

The sliding surface of the LCL GTI typically comprises a linear combination of variables that encompasses the inverter current error, the capacitor voltage error, the grid current error, as well as their respective integrals or derivatives [4]. Some studies have utilized a mixture of the virtual resistor methodology and SMC for LCL damping, while others have not [3], [9], [10]. In contrast, [7] put forth various resonant factors for the sliding surface, excluding supplementary damping techniques. To reduce the cost and required sensor, several state observers proposed to estimate variables in the sliding function [3], [10].

Due to the promising performance of SMCs in dealing

with variable structure systems and uncertainties, SMCs can be associated with a PR controller for current control as well as active resonance damping in an LCL-filtered voltage source inverter connected to a distorted grid. The power quality problems could be considered are voltage swell, voltage sag and unbalanced voltage. In addition, a STSMO is proposed to reduce the sensor requirement. The proposed STSMO-based SMC strategy with a PR controller GTI in an unbalanced grid has desired dynamic as well as high robustness. The simulations carried out in Matlab/Simulink show the effectiveness of the proposed method in current control and resonance suppression even in the presence of voltage fluctuations and parameter variations.

The rest of the paper is organized as follows. In Sec. II, a brief modeling of GTI with LCL filter is presented. The SMC and PR controllers are introduced and designed in Secs. III and IV, while the proposed STSMO is presented in Sec. V. Some selected simulation results are presented in Sec. VI, and the paper is concluded in Sec. VII.

II. State-space Modeling of GTI with LCL Filter

Fig. 1 depicts the structure of a three-phase VSI GTI with an LCL filter. The LCL filter is interfaced by the inverter-side inductor L_1, the filter capacitor C and the grid-side inductor L_2. The resistances r_1, r_2 are the equivalent parasitic series resistances of inductors L_1 and L_2, respectively. The VSI includes six switching devices that are controlled by generated signal from the controller. The VSI state-space equations can be written from the circuit as follows:

$$L_1 \frac{di_1}{dt} + r_1 i_1 = \Gamma u V_{dc} - v_c \tag{1}$$

$$L_2 \frac{di_2}{dt} + r_2 i_2 = v_c - v_g \tag{2}$$

$$C \frac{dv_c}{dt} = i_1 - i_2 \tag{3}$$

Where $\Gamma = \frac{1}{6}\begin{bmatrix} 2 & -1 & -1 \\ -1 & 2 & -1 \\ -1 & -1 & 2 \end{bmatrix}$ in equation (1),and $i_1 = [i_{1a}\ i_{1b}\ i_{1c}]^T$, $i_2 = [i_{2a}\ i_{2b}\ i_{2c}]^T$, $v_c = [v_{ca}\ v_{cb}\ v_{cc}]^T$, and $v_{gk}(t) = V_g \cdot \cos(\omega t + \phi_k)$ with ϕ_k taken as 0, $-2\pi/3$, and $-4\pi/3$ for phases a, b and c, respectively. Also, $u = [u_a\ u_b\ u_c]^T$

$$u_k = \begin{cases} 1, & upper\ q\ closed \\ -1, & lower\ q\ closed \end{cases} \quad and\ k = a, b, c \tag{4}$$

and the reference of i_{2k} should be defined as

$$i_{2k}^*(t) = I_2^* \cdot cos(\omega t + \phi_k + \theta) \tag{5}$$

III. Proposed SMC and Its Existence Condition

Three system dynamics errors are defined as follows:

$$x_1 = v_c^* - v_c \tag{6}$$

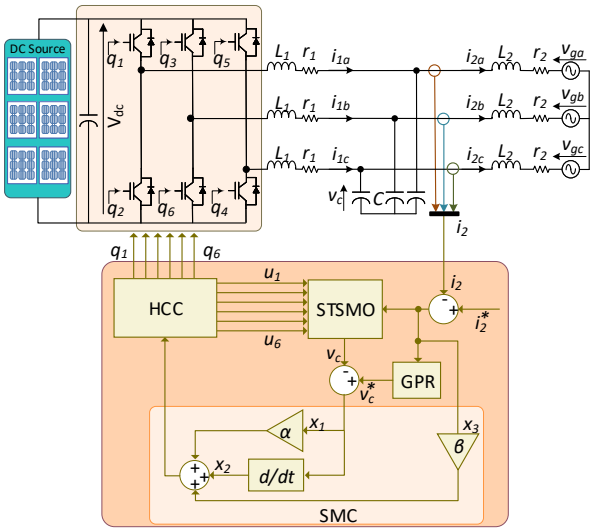

Fig. 1: Three-phase LCL-filtered GTI with the proposed control scheme.

$$x_2 = \dot{v}_c^* - \dot{v}_c \tag{7}$$

$$x_3 = i_2^* - i_2 \tag{8}$$

Where i_2^* is the reference vector of i_2 which is generated by using a user-defined function, then the generation of v_c^* will be discussed in Section (IV). The sliding surface function can be defined as

$$S = \alpha x_1 + x_2 + \beta x_3 \tag{9}$$

Where α and β denote positive constants of dynamic errors. As studied in [9], the $\beta x_3 = \frac{\beta}{L_2}\int x_1 dt$ in (9) mitigates the steady-state errors in v_c and i_2. In the sliding regime, the converter dynamics are compelled to slide over the sliding surface. The requirement in the design of SMC is to satisfy the reaching conditions. The well-known reaching conditions is

$$S\dot{S} < 0 \tag{10}$$

Take the derivative time of S

$$\dot{S} = \alpha \dot{x_1} + \dot{x_2} + \beta \dot{x_3} \tag{11}$$

according to (6) and (7), the derivative x_1 can be obtained

$$\dot{x_1} = x_2 \tag{12}$$

By substituting (3) into (7) gives us

$$x_2 = \frac{dv_c^*}{dt} - \frac{dv_c}{dt} = \frac{dv_c^*}{dt} - \frac{1}{C}(i_1 - i_2) \tag{13}$$

Taking derivative of (13) results in

$$\dot{x_2} = \frac{d^2 v_c^*}{dt^2} - \frac{1}{C}\left(\frac{di_1}{dt} - \frac{di_2}{dt}\right) \tag{14}$$

By substituting (1) and (2) into (14) and then substituting i_1 instead of $i_2 + C\frac{dv_c}{dt}$ yields:

$$\dot{x_2} = \frac{d^2 v_c^*}{dt^2} - \frac{1}{L_1 C}\Gamma u V_{dc} + \frac{1}{L_1 C} v_c + \frac{r_1}{L_1 C} i_2 + \frac{r_1}{L_1 C}\frac{dv_c}{dt} + \frac{1}{L_2 C} v_c - \frac{1}{L_2 C} v_g - \frac{r_2}{L_2 C} i_2 \quad (15)$$

By replacing dv_c/dt using (13) and after some simplifications on (15) finally get:

$$\dot{x_2} = -\omega_1^2 \Gamma u V_{dc} - \omega_r^2 x_1 - \frac{r_1}{L_1} x_2 + (r_2\omega_2^2 - r_1\omega_1^2) x_3 + D \quad (16)$$

Where $\omega_1 = \frac{1}{\sqrt{L_1 C}}$, $\omega_2 = \frac{1}{\sqrt{L_2 C}}$, $\omega_r = \sqrt{\frac{L_1 + L_2}{L_1 L_2 C}}$ and D is a disturbance term which can be obtained from

$$D = \frac{d^2 v_c^*}{dt^2} + \frac{r_1}{L_1}\frac{dv_c^*}{dt} + \omega_r^2 v_c^* - (r_2\omega_2^2 - r_1\omega_1^2) i_2^* - \omega_2^2 v_g \quad (17)$$

For obtaining x_3 we should get derivative from (8)

$$\dot{x_3} = \frac{di_2^*}{dt} - \frac{di_2}{dt} \quad (18)$$

And substitute $\frac{di_2}{dt}$ and $\frac{di_2^*}{dt}$ by introducing (2) into (18)

$$\dot{x}_3 = \frac{r_2}{L_2} x_3 - \frac{1}{L_2} x_1 \quad (19)$$

Since in sliding mode $S = 0$ and $\dot{S} = 0$, thus from (11) we can obtain

$$\dot{x}_2 = -\alpha \dot{x}_1 - \beta \dot{x}_3 \quad (20)$$

By replacing (19) into (20) and using (12) yields

$$\ddot{x}_1 + \alpha \dot{x}_1 - \frac{\beta}{L_2} x_1 = -\beta \frac{r_2}{L_2} x_3 \quad (21)$$

Equation (21) is a second-order non-homogeneous differential equation and when x_3 decreases to zero in a steady-state condition, the equation becomes homogeneous, and x_1 reduces exponentially at a rate defined by α and β. The variable v_c is targeted to reach v_c^* under all circumstances until the sliding mode operation is valid. Now, let's define the control variable

$$u = -sign(S) \quad (22)$$

By using (22) and (10), the existing condition is obtained:

1) When $S < 0 \Rightarrow u = 1$;

$$-\left(\omega_r^2 + \frac{\beta}{L_2}\right) x_1 + \left(\alpha - \frac{r_1}{L_1}\right) x_2 + \left(r_2\omega_2^2 - r_1\omega_1^2 + \frac{\beta r_2}{L_2}\right) x_3 - \omega_1^2 \Gamma u V_{dc} + D > 0 \quad (23)$$

2) When $S > 0 \Rightarrow u = -1$;

$$-\left(\omega_r^2 + \frac{\beta}{L_2}\right) x_1 + \left(\alpha - \frac{r_1}{L_1}\right) x_2 + \left(r_2\omega_2^2 - r_1\omega_1^2 + \frac{\beta r_2}{L_2}\right) x_3 - \omega_1^2 \Gamma u V_{dc} + D < 0 \quad (24)$$

Equations (23) and (24) contain the existing region border of SMC. To avoid high-frequency switching and improve the chattering effect of SMC, a hysteresis function is proposed with a sign function.

$$u = \begin{cases} 1, & S < -h \\ -1, & S > +h \end{cases} \quad (25)$$

Where $+h$ and $-h$ are the higher and lower band of hysteresis function.

IV. Generation of v_c^* by PR Controller

There are two ways to generate v_c^*, one way to derive it by (2) which needs the knowledge of the values of grids voltage, the inductance at grid side and its parasitic resistor. Also, generating (2) needs a derivative operation, which is not favorable in the control loop. Therefore, accurate estimation of this parameter is roughly not possible, and it can make a steady-state error in estimating v_c^*. Another way to generate the reference of the capacitor voltage is PR controller. PR controllers can track an AC signal well with zero steady-state error. Therefore, this important feature of the PR controller can be used to generate v_c^* so that there is no steady state error in the grid current. Now, if the network current error $(i_2^* - i_2)$ is applied to the input of our PR controller, the output of the PR controller will be v_c^* and in this case, i_2 has to follow i_2^*. The transfer function of PR controller is given as

$$G_{PR}(s) = K_p + \frac{2K_i\omega_c s}{s^2 + 2\omega_c s + 2\omega_0^2} \quad (26)$$

Where K_p is the proportional gain and K_i is the resonant gain, ω_c and ω_0 are respectively the cutoff angular frequency and the fundamental angular frequency [11].

V. Super Twisting Sliding Mode Observer (STSMO)

To reduce the number of sensors and increase the stability of the system, we plan to implement a super-twisting sliding observer method so that it can estimate the capacitor voltage.

A. Observer model and observability

Considering that the variables i_1, i_2 and v_c are the system state variables and defining v_c as the output of the system and using the equations (1) to (3) yields the following state space

$$\begin{cases} \dot{x}_k = Ax_k + Bu_k + D \\ y_k = Cx_k \end{cases} \quad (27)$$

Where

$$x_k = \begin{bmatrix} i_{1k} \\ i_{2k} \\ v_{ck} \end{bmatrix} \quad A = \begin{bmatrix} -\frac{r_1}{L_1} & 0 & -\frac{1}{L_1} \\ 0 & -\frac{r_2}{L_2} & -\frac{1}{L_2} \\ \frac{1}{C} & -\frac{1}{C} & 0 \end{bmatrix}$$
$$B = \begin{bmatrix} \frac{V_{dc}}{L} \\ 0 \\ 0 \end{bmatrix} \quad D = \begin{bmatrix} 0 \\ -\frac{v_{gk}}{L_2} \\ 0 \end{bmatrix} \quad C = \begin{bmatrix} 0 \\ 0 \\ 1 \end{bmatrix} \quad (28)$$

Where $k = \{a, b, c\}$. An essential condition for observer design is system visibility. According to the equation (29), the $Obsv$ matrix is full rank and the system is observable.

$$Obsv(A, C) = \begin{bmatrix} C \\ CA \\ CA^2 \end{bmatrix} \quad \text{and} \quad rank\big(Obsv(A, C)\big) = 3 \tag{29}$$

B. STSMO design

Considering the response time and reducing the level of chattering, a sliding model observer is designed according to the following equations.

$$\begin{cases} \dot{\hat{x}}_k = A\hat{x}_k + Bu_k + \lambda(y_k - \hat{y}_k) + \gamma|y_k - \hat{y}_k|^{(p-1)} sign(y_k - \hat{y}_k) \\ \hat{y}_k = C\hat{x}_k \end{cases} \tag{30}$$

Where $\hat{x} = [\hat{i}_{1k} \ \hat{i}_{2k} \ \hat{v}_{ck}]^T$, which are estimated values of i_{1k}, i_{2k} and v_{ck}, respectively. $\lambda = [\lambda_1 \ \lambda_2 \ \lambda_3]^T$ $(\lambda_i > 0, \ i = 1, 2, 3)$ is the matrix of observer coefficients, $\gamma = [\gamma_1 \ \gamma_2 \ \gamma_3]^T$ $(\gamma_i > 0, \ i = 1, 2, 3)$ is a constant matrix and $|y_k - \hat{y}_k|^{p_1}$ $(0 < p_1 < 1)$ is gain of switching function. By subtracting the expression (30) from (27), the observer error equation will be obtained

$$\dot{e} = A_0 e + \gamma|y - \hat{y}|^{p_1} sign(y - \hat{y}) \tag{31}$$

Where $e = x - \hat{x}$ is observer error and $A_0 = A - \lambda C$. A large value of $|y - \hat{y}|^{p_1}$ can increase the response speed of the STSMO, while small values can mitigate the chattering level so that the observer can operate quickly and satisfactorily.

C. Stability of STSMO

The Lyapunov Function is used to prove the stability of the STSMO. Here the Lyapunov candidate function is the following function

$$V = e^T P e \tag{32}$$

where P is the solution of the Lyapunov equation (33) which must be a positive symmetric matrix.

$$A_0^T P + P A_0 = -Q \tag{33}$$

And Q must also be a positive symmetric matrix. If we take a derivative of relation (32) along with (31) we obtain

$$\begin{aligned} \dot{V} =& \dot{e}^T P e + e^T P \dot{e} \\ =& \big(A_0 e - \gamma|y - \hat{y}|^{p_1} sign(y - \hat{y})\big)^T + \\ & P[A_0 e - \gamma|y - \hat{y}|^{p_1} sign(y - \hat{y}] \\ =& e^T(PA_0 + A_0^T P)e - |y - \hat{y}|^{p_1} sign(y - \hat{y}) \\ & \cdot \big(\gamma^T P e + e^T P \gamma\big) \end{aligned} \tag{34}$$

By substituting (34) into (33) we have

$$\begin{aligned} \dot{V} =& - e^T Q e - |y - \hat{y}|^{p_1} sign(y - \hat{y})[Ce + (Ce)^t] - \\ & e^T Q e - 2|y - \hat{y}|^{p_1} sign(y - \hat{y})(y - \hat{y}) \\ =& -e^T Q e - 2|y - \hat{y}|^{p_1 + 1} \end{aligned} \tag{35}$$

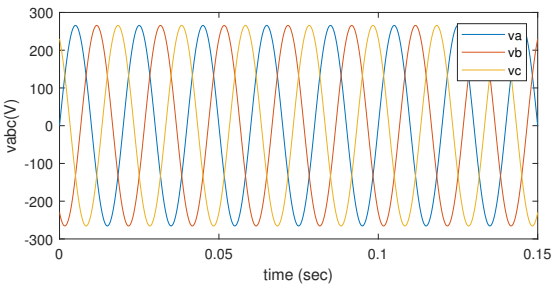

(a)

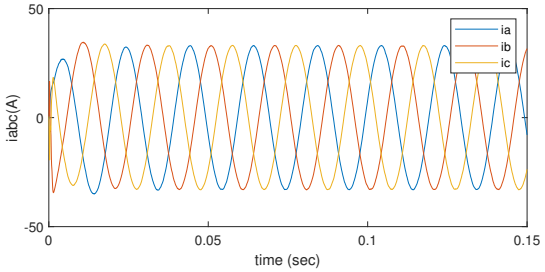

(b)

Fig. 2: Steady-state waveforms of GTI (a) voltage (v_{ga}, v_{gb}, v_{gc}) and (b) current(i_{2a}, i_{2b}, i_{2c}).

Clearly, $\dot{V} < 0$ in equation (35) when e is non-zero. According to Lyapunov's stability theory, the error of the observer of the system (35) is asymptotically stable, and this means that the error of the observer of the system e decays to zero ($\hat{i_1} \longrightarrow i_1$, $\hat{i_2} \longrightarrow i_2$, $\hat{v_c} \longrightarrow v_c$).

VI. SIMULATION RESULTS

To evaluate the effectiveness of the proposed system shown in Fig. 1 some simulations are carried out in the Matlab/ Simulink software environment and the parameters of the system are presented in Table I. In this control structure, STSMO plays the role of our observer to estimate the capacitor voltage. The G_{PR} block, which represents the PR controller, is used to generate the capacitor voltage reference.

TABLE I: SYSTEM PARAMETERS

System Parameter	symbol	value
DC link voltage	V_d	700 Vdc
Grid voltage	V_g	230 V(RMS)
Grid frequency	f_g	50 Hz
Sample rate		2 μs
Inverter side inductance	L_1	1.74 mH
Grid side inductance	L_1	0.68 mH
Filter capacitance	C	10 μF
Inductor resistance	$r_{1,2}$	0.2 Ω
Coefficients of SMC	α, β	4300, 13×10^3
Coefficients of STSMO	λ	[9 0.5 5]×10^6
	γ	[5 0.05 5]×10^6
	p_1	[0.5 0.9 0.9]

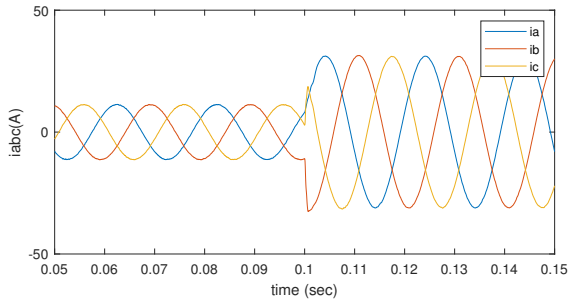

Fig. 3: Grid current (i_{2a}, i_{2b}, i_{2c}) responses to the variation of reference grid current.

In Fig. 2, it can be seen that the proposed system has a decent steady-state performance and the grid current and voltage are in the same phase all the time. Moreover, the LCL filter perfectly filters out the switching harmonics and no resonance is seen in the grid current.

To evaluate the tracking performance of the controller, a step change is considered on the current reference value and the results are shown in Fig. 3. It is supposed that at $t = 0.1$s the set point of the current changes suddenly from 12A to 32A. Fig. 3 shows that the proposed controller responses in a reasonable time and tracks the reference value.

To evaluate the robustness against the variation of the model parameters two simulations are done in which the value of the grid side inductance is considered to be changed, in the former case it is 0.408 mH and in the latter case it is 1.36 mH. Fig. 4 shows the robustness against decreasing and increasing of grid inductance variations. In Fig. 4a the THD of the grid current is 0.59% and in Fig. 4b it is 1.05%. It can be seen that the THD remains in a reasonable range though the inductances don't have nominal values.

The proposed controller can also operate in the case of unbalanced grid voltage. Fig. 5 shows the VSI performance under the unbalanced grid voltage. For this test, the phase A amplitude was reduced by 20%. It worth mentioning that the use of a specific PLL algorithm for extracting the positive and negative sequences of the grid voltage is not necessary in this case. THD is 1.54% which still meets the requirements as per IEEE.Std519-2014. Moreover, without STSMO THD is 1.05% which approves that the proposed observer does not have substantial negative effect on the THD in an unbalanced grid.

The controller is capable of functioning even in the presence of voltage sags. As depicted in Fig. 6, there was a 20% reduction in the grid voltage from $t = 0.05$s to $t = 0.1$s. Nonetheless, the amplitude of the grid side current remained constant during this time interval. The THD of the grid side was determined to be 0.34%, which is as normal operational state.

Fig. 7 illustrates the spectrum of the control signal. Despite the utilization of hysteresis modulation, it is observed that the spectrum is primarily concentrated at a frequency of approximately 14 kHz.

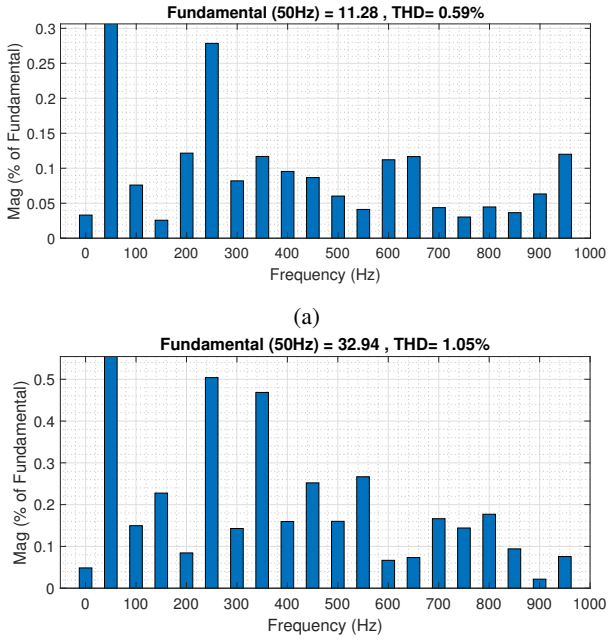

Fig. 4: Fast Fourier Transform of Grid-side currents (i_2) for two different values of L_2: (a) 100% increase and (b)40% decrease.

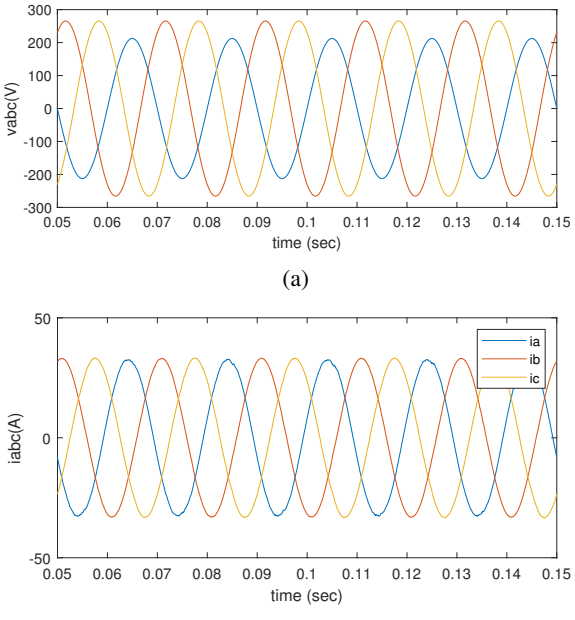

Fig. 5: VSI under unbalanced Grid (a) Grid Voltage (v_{ga}, v_{gb}, v_{gc}), (b) Grid side current (i_{2a}, i_{2b}, i_{2c}).

VII. CONCLUSION

In this study, a sliding-mode and proportional-resonant (PR) based control strategy for three-phase grid-connected LCL-filtered voltage source inverters (VSI) with super twisting

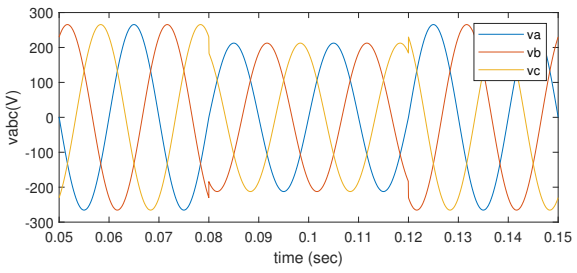

(a)

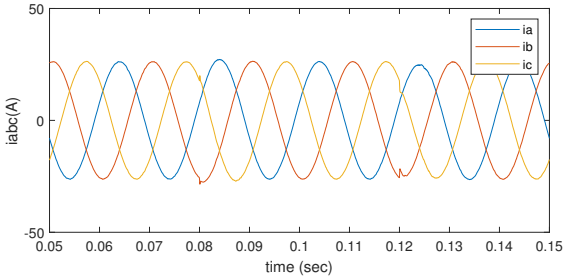

(b)

Fig. 6: Test under voltage sags (a) grid voltage (v_{ga}, v_{gb}, v_{gc}) (b) grid side current(i_{2a}, i_{2b}, i_{2c}).

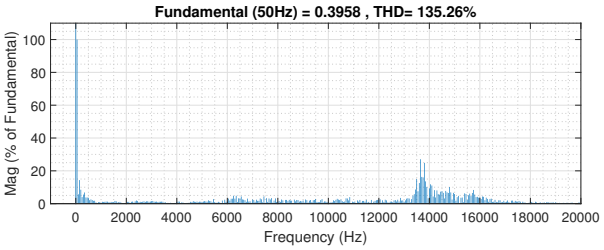

Fig. 7: Switching signal spectrum.

sliding mode is proposed. The generation of the three-phase reference capacitor voltages is highlighted as a critical component of the proposed control strategy. To overcome the need to employ a derivative operation and to eliminate steady-state errors in the grid current, a PR controller is used to generate the capacitor reference voltages, making the system independent of the grid inductance. Simulation analysis demonstrates that the controller is able to operate optimally at the designated operational points. Additionally, the STSMO also presents a satisfactory outcome in the established operational points.

REFERENCES

[1] "Ieee recommended practice and requirements for harmonic control in electric power systems," *IEEE Std 519-2014 (Revision of IEEE Std 519-1992)*, pp. 1–29, 2014.

[2] R. Teodorescu, F. Blaabjerg, M. Liserre, and A. Dell'Aquila, "A stable three-phase lcl-filter based active rectifier without damping," in *38th IAS Annual Meeting on Conference Record of the Industry Applications Conference, 2003.*, vol. 3, 2003, pp. 1552–1557 vol.3.

[3] R. Guzman, L. G. de Vicuña, J. Morales, M. Castilla, and J. Miret, "Model-based active damping control for three-phase voltage source inverters with lcl filter," *IEEE Transactions on Power Electronics*, vol. 32, no. 7, pp. 5637–5650, 2017.

[4] M. Huang, H. Li, W. Wu, and F. Blaabjerg, "Observer-based sliding mode control to improve stability of three-phase lcl-filtered grid-connected vsis," *Energies*, vol. 12, no. 8, 2019. [Online]. Available: https://www.mdpi.com/1996-1073/12/8/1421

[5] R. Teodorescu, F. Blaabjerg, M. Liserre, and P. C. Loh, "Proportional-resonant controllers and filters for grid-connected voltage-source converters," *IEE Proceedings-Electric Power Applications*, vol. 153, no. 5, pp. 750–762, 2006.

[6] X. Zheng, K. Qiu, L. Hou, Z. Liu, and C. Wang, "Sliding-mode control for grid-connected inverter with a passive damped lcl filter," in *2018 13th IEEE Conference on Industrial Electronics and Applications (ICIEA)*, 2018, pp. 739–744.

[7] X. Hao, X. Yang, T. Liu, L. Huang, and W. Chen, "A sliding-mode controller with multiresonant sliding surface for single-phase grid-connected vsi with an lcl filter," *IEEE Transactions on Power Electronics*, vol. 28, no. 5, pp. 2259–2268, 2013.

[8] V. I. Utkin, *Sliding Modes and Their Applications in Variable Structure Systems*. Mir Publishers, 1978. [Online]. Available: https://hal.science/hal-00848243

[9] H. Komurcugil, S. Ozdemir, I. Sefa, N. Altin, and O. Kukrer, "Sliding-mode control for single-phase grid-connected LCL-filtered vsi with double-band hysteresis scheme," *IEEE Transactions on Industrial Electronics*, vol. 63, no. 2, pp. 864–873, 2016.

[10] R. Guzman, L. G. de Vicuña, M. Castilla, J. Miret, and H. Martín, "Variable structure control in natural frame for three-phase grid-connected inverters with lcl filter," *IEEE Transactions on Power Electronics*, vol. 33, no. 5, pp. 4512–4522, 2018.

[11] H. Cha, T.-K. Vu, and J.-E. Kim, "Design and control of proportional-resonant controller based photovoltaic power conditioning system," in *2009 IEEE Energy Conversion Congress and Exposition*, 2009, pp. 2198–2205.